

## Susceptibility of the Surrounding Soil and Rock by the Electrical Resistivity Method

Ratna Husain\*, Sultan

Department of Geology, Faculty of Engineering, Hasanuddin University, Makassar, Indonesia

\*Corresponding author. Email: [ratna7geologi@gmail.com](mailto:ratna7geologi@gmail.com)

Manuscript received: 7 November 2022; Received in revised form: 26 January 2023; Accepted: 14 February 2023

### Abstract

The research area is located in Banga, Soppeng Regency, South Sulawesi Province. The purpose and intent of this research is to determine the resistivity value of the material layer, identify the characteristics of the slip plane and its relationship to the plasticity properties and the characteristics of the clay minerals contained in the soil. The method used to collect field data includes surface geological data and subsurface geology, which are the electrical resistivity data and surface soil data, then interpreted by combining topographic cross-sectional data and subsurface geoelectrical data along the measurement path. The first slip plane is curved as well as the second slip plane is the residual soil resulting from weathering of limestone which is still above the less dense and thick parent rock (in situ). The geochemistry of the soil samples showed that the mineral content in each layer had the largest percentage of illite 54.4% - 69.9%, and montmorillonite 6.1% - 13.6%, these two clay minerals have large shrinkage properties. Plasticity Index 29.8% - 35.8%, causing vulnerability to the soil, so that the mass movement on the sliding plane is moderate and active in slow motion. The mass movement in the slip plane can be categorized into creep type.

**Keywords:** plasticity index; resistivity; slip plan; XRD.

**Citation:** Husain, R. & Sultan. (2023). Susceptibility of the Surrounding Soil and Rock by the Electrical Resistivity Method. *Jurnal Geocelebes*, 7(1), 29-36, doi: 10.20956/geocelebes.v7i1.23889

### Introduction

The Banga area is a place for sampling soil and geoelectric data, mostly steep topography, which is traversed by connecting roads from Makassar to Soppeng Regency and from Soppeng Regency to Makassar. This road section often suffers from cracks and damage to the road body and certain parts collapse, so attention is needed from the local government, so that landslide – prone locations can be anticipated so as not to cause a disaster.

Several studies to determine the slip plane using the geoelectric method have been carried out such as Permanasari et al. (2020) and Tejakusuma (2020), but this study tries to relate the soil and mineral

content contained as a result of weathering of the bedrock whether it plays an important role in the occurrence of landslide both on a large and small scale.

One of the factors that influence the cause of ground motion is the presence of a sliding plane or a shear plane. Generally, avalanches will occur above the slip plane so that the layers of soil or rock above it can move. Several methods can be used to identify slip planes, one of which is the resistivity geophysical method. The geoelectric method has the advantage that it is safe for the environment, low cost, and the type of soil layer can be recorded to great depths (Aweda et al., 2023; Bamerni and Mohammed, 2023), so this method is used in surveys to obtain subsurface data. The thickness of soil and clay minerals,

which have expansive properties, also contributes to the soil becoming plastic (Husain, 2015).

In addition to the presence of slip planes, weathering of bedrock factors can produce different minerals contained in the soil, so that soil properties can be determined depending on the minerals formed during the weathering process of the original rock (Husain et al., 2015).

Limestone (Figure 1) is the main constituent rock of the Banga area (Sukanto, 1982), is widely distributed and occupies the high-altitude area of the study site. The megascopic appearance of fresh grayish white color and blackish brown weathered color, consisting of grain, sparite, micrite in the form of calcite minerals is called Packstone (Dernaika et al., 2023).



**Figure 1.** Limestone outcrop.

Soil derived from weathered rocks that have undergone chemical and physical weathering, which does not undergo displacement in the parent rock, is called residual soil (Sudarsono and Hasibuan, 2011), showing a dry brown color and a blackish brown color when wet.

## Methods

The location for collecting geoelectric data (Figure 2), as well as for soil samples is carried out at coordinates between  $04^{\circ}29'49''$  S –  $04^{\circ}31'18''$  S and  $119^{\circ}49'53''$  E –  $119^{\circ}51'23''$  E.

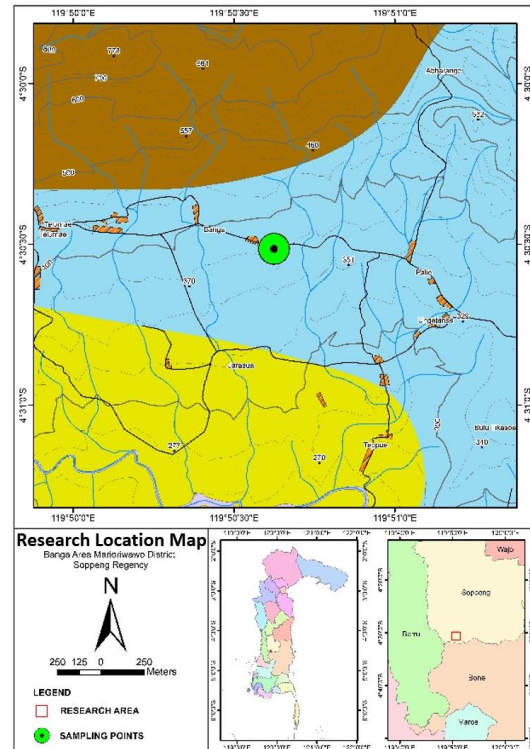


**Figure 2.** Location of sampling.

Preparation of equipment used in GPS surveys, a Brunton compass, a unit of resistivity meter and its accessories, and application program software, GIS (ArcGIS 9.3 MapsSource Garmin, Surfer 11 and Global Mapper 13) and resistivity application program (GeoRes v3. b14) and Res2DInv.

The analyzed data is correlated between rock resistivity and geological factors, then converted from subsurface rock resistivity, so that the mineral resistivity value can be known (Martorana and Capizzi, 2023; Shanshal and Al-Mashhadany, 2023) and the type of subsurface material (Adam et al., 2023; Almeida et al., 2023). The resistivity measurement results are analyzed to obtain subsurface rocks, based on these values produce a two-dimensional profile image.

Soil samples were taken using a hand auger at a depth so shallow that it could not be taken by the tool. Then the soil was analyzed using the XRD method to determine the mineral composition

contained in the soil. Soil samples were taken using a hand drill at a depth so shallow that it could not be taken by the tool. Then the soil was analyzed using the XRD method to determine the mineral composition contained in the soil.

## Results and Discussion

Data collection using a multichannel geoelectric device with a Wenner configuration (Bundang et al., 2022; Amsah and Umar, 2020), measurements were carried out using a stretch length of 150 m, electrode distance of approximately 10 m. In this area there is evidence of ground movement, there are cracks above the highway and the road body is partially broken, the dimensions of the cracked road are 25 meters long, 5 meters high, 18o slope and 1-meter-thick soil. Dry brown soil and blackish brown wet soil, medium plant vegetation and crushed limestone.

The data obtained after the apparent resistivity calculation is inverted with the Res2Dinv program. The result of the program inversion is a 2-dimensional resistivity cross-section (Aryadi, 2014), which can be seen in Figure 3. The interpretation of the lithological cross section based on the resistivity value.

The data analysis produces variations in the resistivity value from 0.1 m to 274 m, it can be interpreted that there is an accumulation of water mixed with residual soil with a resistivity value of 0.1 m - 45.5 m. Located on the 15th to 135th meters with a depth of 2.5-31.9 meters. The reason for the existence of the layer below is an impermeable rock layer where the nature of this layer is very difficult for water to pass. Furthermore, there is a second layer which has a resistivity value of 45.6 m - 100 m, which is interpreted as a layer of non-resistant limestone and mixed with clay-sized soil (clays). This layer also contains water caused by the lack of water in the soil layer because the rock layers below are not impermeable to water. Located at the 23rd to 60th meters and 58th to 125th meters at a depth of 2.5 to 10 m.

The lowest layer is the rock layer with the highest resistivity value of 100.1  $\Omega\text{m}$  - > 274  $\Omega\text{m}$ . The resistivity value can be interpreted as a layer of limestone (Azis et al., 2023; Rahmaniah et al., 2021). Located at 74 – 112 meters with a depth of 12.5 – 31.9 meters.

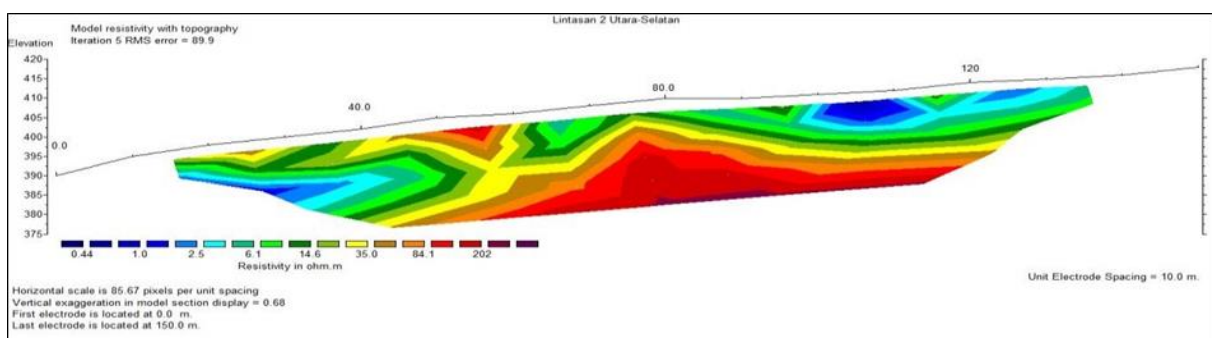


**Figure 3.** Geoelectric inverse section.

### *Slip plan analysis*

Analysis of landslides that may occur above the slip plane can be determined based on field data processing in the form of surface data which is then combined with subsurface data from the results of

geoelectrical analysis. Field data and geoelectrical data in an area are used to determine the direction of the avalanche slip plane. Field data and geoelectrical data in an area are used to determine the direction of the avalanche slip plane. Before carrying out the analysis of

determining the slip plane, it must first be known that places that are prone to ground motion can be seen from the slope, geomorphology, and constituent rocks.

The interpretation of the geoelectrical resistivity inversion section shows the presence of a slip plane on this line. The low resistivity value is between the higher resistivity values to form a slip plane. This layer is easy to flow and erodes, layers with low resistivity values (0.1 m - 45.5 m) are residual soil as a result of weathering of sedimentary rocks, which is limestone with resistivity values of 100.1 m - 274 m as source rock (in situ). less dense and thick.

The first slip plane was found at the 85th meter to the 43rd meter with a depth of 2.5 meters to a depth of 20 meters. The direction of the slip plane relative to North to South is in the direction of the slope of the rock layers.

#### *XRD analysis test*

The weathering process will change the rock or dissolve some minerals so that it becomes soil, then transported and deposited as unconsolidated sedimentary rock. Some minerals dissolve completely and form new minerals. Soil composition does not only depend on the source rock (origin), they are all influenced by nature, intensity, and duration (length of time), weathering and the soil type depend on weathering process (Vieira et al., 2020). In chemical weathering water and dissolved gases play a very important role, while chemical weathering itself has the most important role in all types of weathering. This is why in the study of soil or clastic rock it has a mineral composition that can be very different from the rock of origin.

The results of the XRD analysis on the top layer contained the following minerals (Figure 4):

- Illite ( $\text{Al}_4\text{KO}_{12}\text{Si}_2$ ): 69.9%
- Vermiculite ( $\text{H}_2\text{Mg}_3\text{O}_{12}$ ) 14.6%

- Chlorite ( $\text{H}_4\text{Mg}_3\text{O}_9\text{Si}_2$ ) 9.4%
- Montmorillonite ( $\text{Al}_2\text{CaO}_{12}\text{Si}_4$ ) 6.1%
- Kaolinite ( $\text{Al}_2\text{H}_4\text{O}_9\text{Si}_2$ ) 0.0%
- Aluminium silicate hydroxide ( $\text{Al}_2\text{H}_8\text{O}_{11}\text{Si}_2$ ) 0.0%

The results of the XRD analysis on the middle layer contained the following minerals (Figure 5):

- Illite ( $\text{Al}_4\text{KO}_{12}\text{Si}_2$ ): 54.4%
- Vermiculite ( $\text{H}_2\text{Mg}_3\text{O}_{12}$ ) 18.3%
- Chlorite ( $\text{H}_4\text{Mg}_3\text{O}_9\text{Si}_2$ ) 13.7%
- Montmorillonite ( $\text{Al}_2\text{CaO}_{12}\text{Si}_4$ ) 13.6%
- Kaolinite ( $\text{Al}_2\text{H}_4\text{O}_9\text{Si}_2$ ) 0.0%
- Aluminium silicate hydroxide ( $\text{Al}_2\text{H}_8\text{O}_{11}\text{Si}_2$ ) 0.0%

The results of the XRD analysis on the bottom layer contained the following minerals (Figure 6):

- Illite ( $\text{Al}_4\text{KO}_{12}\text{Si}_2$ ): 65.5%
- Vermiculite ( $\text{H}_2\text{Mg}_3\text{O}_{12}$ ) 22.6%
- Montmorillonite ( $\text{Al}_2\text{CaO}_{12}\text{Si}_4$ ) 9.1%
- Chlorite ( $\text{H}_4\text{Mg}_3\text{O}_9\text{Si}_2$ ) 2.5%
- Kaolinite ( $\text{Al}_2\text{H}_4\text{O}_9\text{Si}_2$ ) 0.0%
- Aluminium silicate hydroxide ( $\text{Al}_2\text{H}_8\text{O}_{11}\text{Si}_2$ ) 0.0%

#### *Atterberg analysis test*

Classification of plasticity index and soil type, according to Table 1:

**Table 1.** Plasticity index value and soil type (Chen, 1988; Keskin et al., 2023).

PI	Property	Soil Type
0	Non plastics	Sand
< 7	Low plasticity	Silt
7 – 17	Medium plasticity	Silty clay
> 17	High plasticity	Clay

The results of data processing to determine the Atterberg test on the upper layer have a liquid limit value (LL) of 82.80%; plastic limit (PL) 50.02%; Plasticity index (PI) 32.78%. The Atterberg test on the middle layer has a liquid limit value (LL) of 82.80%. plastic limit (PL) 53%; Plasticity index (PI) 29.8%. The Atterberg test on the lower layer has a liquid limit value (LL) of 79.56%; plastic limit (PL) 43.76%, plasticity index (PI) 35.8%.

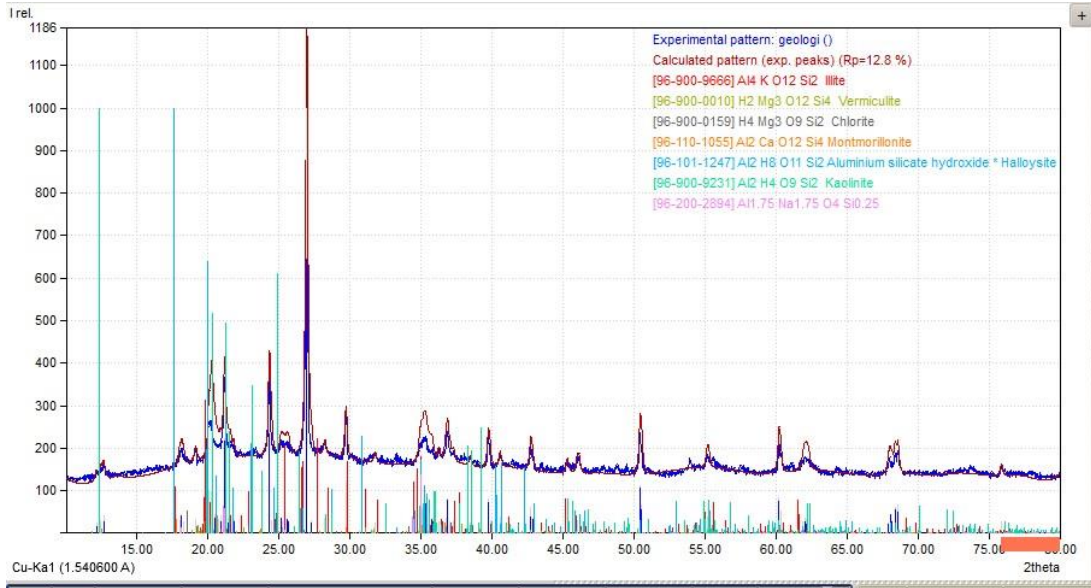


Figure 4. Diffractogram the residual soil of the top layer.

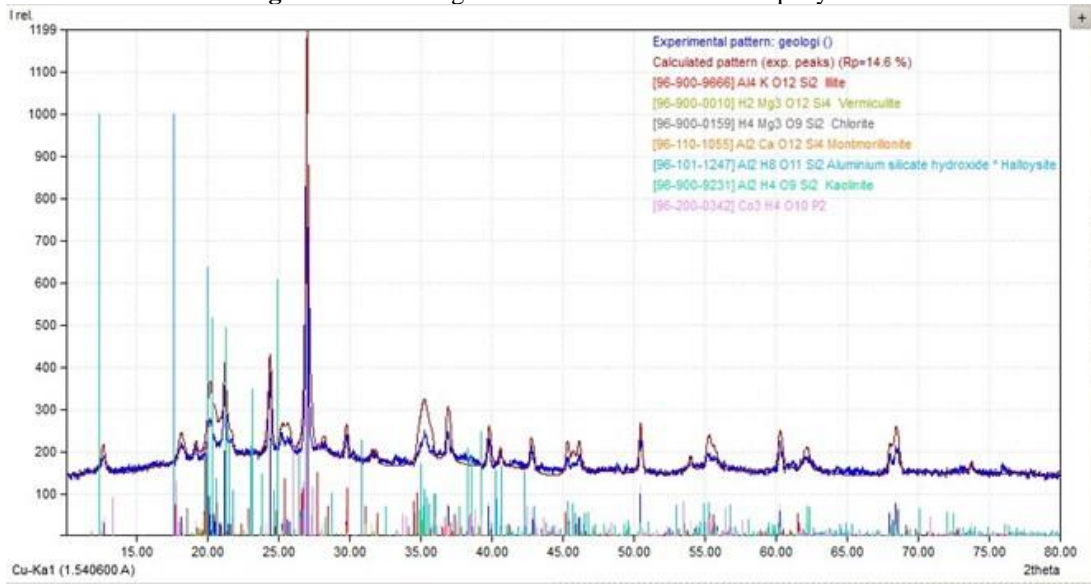


Figure 5. Diffractogram the residual soil of the middle layer.

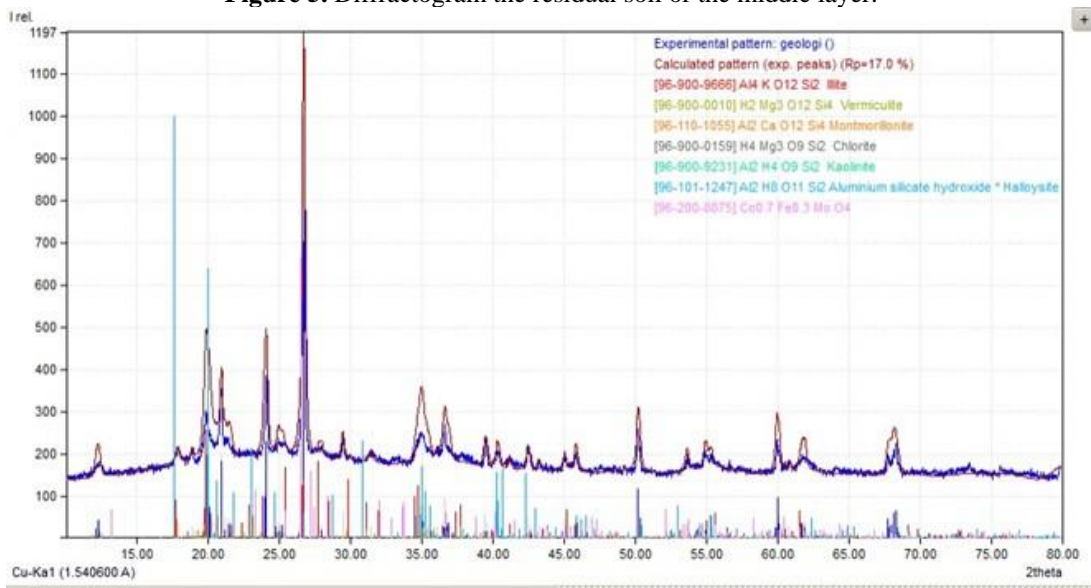


Figure 6. Diffractogram the residual soil of the bottom layer.

The results of the calculation of the plasticity index can be concluded that the type of soil found in the study area is clay with high plasticity > 17% (classification of soil types based on high plasticity index, (Chen, 1988; Keskin et al., 2023)). The stability of the soil or rock that forms a downward slope can cause shear stress to develop intensively so that a slip plane is formed (Guo et al., 2023), explains that the movement occurs along the slip plane asynchronously. Rock fractures as the most influential factor in the process of forming the slip plane in these measurements. This can cause weathering that forms soil. Based on the XRD (X-Ray Diffraction) results on the sample, it shows that clay minerals are the dominant soil component so that a layer of clay is formed. The clay layer will be the infiltration boundary (discontinuous plane), which is the areas in the rock layers that are not continuous.

The clay layer can form an impermeable layer that absorbs a lot of water when there is high rainfall. The accumulation of water will cause the clay layer to expand. (Swelling Potential), if evaporation occurs in the dry season, due to reduced water supply, the clay layer becomes dry, so that the soil layer shrinks (Shrinkage Potential), then the material above it is susceptible to shifting.

### Conclusion

The clay minerals contained in the soil with the highest percentage values were Illite ( $\text{Al}_4\text{KO}_{12}\text{Si}_2$ ) 32.3% - 55.6%, Vermiculite ( $\text{H}_2\text{Mg}_3\text{O}_{12}$ ) 14.6% - 22.6%, Montmorillonite ( $\text{Al}_2\text{CaO}_{12}\text{Si}_4$ ) 6.1% - 18.9%. These clay minerals will cause the soil to become expansive; the soil has a plasticity index value of 21.86% - 26.44%, is a high plastic type of soil.

From the observation of the geoelectric stretch, the slip plane is found at the 85th meter to the 43rd meter with a depth of 1 meter to a depth of 2.5 meters to a depth of

20 meters. Curved shape with residual soil (0.1 m - 45.5 m) which is the result of weathering of limestone (100.1 m - 274 m) and remains on top of the parent rock (in situ). Mass movement will occur on a small-scale sliding plane and is actively moving slowly. Such mass movements are categorized into creep types.

### Acknowledgements

This research was assisted by laboratory staff on the Atterberg test which was carried out in the geotechnical laboratory, Civil Department and XRD analysis was carried out in the laboratory of the Department of Geology, Faculty of Engineering, Hasanuddin University, also thanks to the editors and reviewers for help, correction, and suggestion for our manuscript.

### Author Contribution

Ratna Husain designed and conducted all the experiments and wrote the manuscript. All authors have read and approved of the final manuscript.

### Conflict of Interest

The authors declare that they hold no competing interests.

### References

- Adam, M., Wang, L., Kheiralla, K., Wadi, D., & Ngata, M.R. (2023). Foundation assessment using integrated geophysical techniques for natural gas pipeline route in Al-Sabaloka area, Sudan. *Arabian Journal of Geosciences*, 16(1), 1–16. <https://doi.org/10.1007/s12517-022-11162-7>
- Almeida, H.D., Marques, M.C.G., Sant'Ovaia, H., Moura, R., & Marques, J.E. (2023). Environmental Impact Assessment of the Subsurface in a Former W-Sn Mine: Integration of Geophysical Methodologies.

- Minerals*, 13(1), 55.  
<https://doi.org/10.3390/min13010055>
- Amsah, L.O.M.Y. & Umar, E.P. (2020). Identifikasi Zona Mineralisasi Emas Menggunakan Metode Resistivitas dan Induksi Polarisasi (IP) di Desa Lintidu Kabupaten Buol. *Jurnal Geoelebes*, 4(2), 144–149.  
<https://doi.org/10.20956/geoelebes.v4i2.11126>
- Aryadi, A. (2014). *Identification of the slip plane with the geoelectric method of resistivity in the Gattareng area, Kec. Marioriwawo Kab. Soppeng, South Sulawesi Province*. Universitas Hasanuddin.
- Aweda, A.K., Jatau, B.S., Goki, N.G., Bashir, I.Y., & Obaje, N.G. (2023). Application of VES and 2D Resistivity Methods for Groundwater Exploration in Kutigi-Enagi Region, Northern Bida Basin, Nigeria. *Saudi Journal of Engineering and Technology*, 8(2), 29-40.  
<https://doi.org/10.36348/sjet.2023.v08i02.001>
- Azis, A., Irfan, U.R., & Alimuddin, I. (2023). Geoelectrical resistivity and geochemical method for groundwater investigation in the coastal sediment. *IOP Conference Series: Earth and Environmental Science*, 1134(1), 012020. <https://doi.org/10.1088/1755-1315/1134/1/012020>
- Bamerni, K.D. & Mohammad, R.J. (2023). 2D Resistivity Technique in Exploring Soil Contamination Zones, Kwashe Area, Duhok, North of Iraq. *The Iraqi Geological Journal*, 56(1A), 253–264.  
<https://doi.org/10.46717/igj.56.1A.19ms-2023-1-31>
- Bundang, S., Massinai, M.F.I., Firman, F., & Hidayat, W. (2022). Subsurface Profile Analysis for Aquifer Layer Identification. *Jurnal Geoelebes*, 6(2), 194–202.  
<https://doi.org/10.20956/geoelebes.v6i2.21911>
- Chen. F.H. (1988). *Foundation on Expansive Soils*. Elsevier Scientific Publishing, New York.
- Dernaika, M.R., Masalmeh, S., Mansour, B., Al Jallad, O., & Koronfol, S. (2023). Modeling Permeability in Different Carbonate Rock Types. *Petrophysics*, 64(01), 18–37.  
<https://doi.org/10.30632/PJV64N1-2023a2>
- Guo, Z., Huang, Q., Liu, Y., Wang, Q., & Chen, Y. (2023). Model experimental study on the failure mechanisms of a loess-bedrock fill slope induced by rainfall. *Engineering Geology*, 313, 106979.  
<https://doi.org/10.1016/j.enggeo.2022.106979>
- Husain, R. (2015). *Geochemistry of Clay Mineral and Its Implication Toward landslide*. Hasanuddin University.
- Husain, R., Imran, A.M., Irfan, U.R., & Harianto, T. (2015). Nature and Plasticity of Residual Soil in Relation to the Landslide Susceptibility at Marioriwawo, South Sulawesi. *International Journal of Engineering and Science Applications*, 2(1), 61–67.  
<http://pasca.unhas.ac.id/ojs/index.php/ijesca/article/view/148>
- Keskin, İ., Salimi, M., Ateyşen, E. Ö., Kahraman, S., & Vakili, A.H. (2023). Comparative Study of Swelling Pressure in Expansive Soils considering Different Initial Water Contents and BOFS Stabilization. *Advances in Civil Engineering*, 2023 2023, Article ID 4823843, 11 pages, 2023.  
<https://doi.org/10.1155/2023/4823843>
- Martorana, R. & Capizzi, P. (2023). Evaluation of Artifacts and Misinterpretation in 2D Electrical Resistivity Tomography Caused by Three-Dimensional Resistive Structures of Regular or Irregular Shapes. *Applied Sciences*, 13(3), 2015.  
<https://doi.org/10.3390/app13032015>
- Purnamasari, I.N.P., Ipmawan, V.L., & Khairuman, E. (2020). Determination

- of Slip Surface Using 2D Geoelectric Resistivity Method and Laboratory Analysis for Landslide Prone Area Pesawaran, Lampung. *IOP Conference Series: Earth and Environmental Science*, 537(1), 012011. <https://doi.org/10.1088/1755-1315/537/1/012011>
- Rahmaniah., Wahyuni, A., Massinai, M.F.I., Mun'im, A., & Massinai, M.A. (2021). Resistivity Method for Characterising Subsurface Layers of Coastal Areas in South Sulawesi, Indonesia. *Journal of Geoscience, Engineering, Environment, and Technology*, 6(4), 217–225. <https://doi.org/10.25299/jgeet.2021.6.4.6242>
- Shanshal, Z. M. & Al-Mashhadany, A. Y. (2023). Detection of Soil Contamination Using Electrical Resistivity Tomography and Induced Polarization Methods by Tank Model. *The Iraqi Geological Journal*, 56(1A), 208–220. <https://doi.org/10.46717/igj.56.1A.16ms-2023-1-28>
- Sudarsono, U. & Hasibuan, G. (2011). Engineering Geological Characteristics of the Residual Soil, Lower Quaternary Sediments in Kertajati Region, Majalengka, West Java. *Indonesian Journal on Geoscience*, 6(3), 177–189. <https://doi.org/10.17014/ijog.6.3.177-189>
- Sukamto R. (1982). *Geologi Lembar Pangkajene dan Watampone Bagian Barat, dan Lembar Ujungpandang, Benteng dan Sinjai*. Pusat Survey Geologi, Direktorat Sumber Daya Energi, Mineral dan Pertambangan, Bandung.
- Tejakusuma, G.I. (2020). Determination of Landslide Slip Plane Using Geology and Geoelectrical Analysis at Mount Geger Pulus Legok Emo Slope Segment, Cililin, West Java. *Jurnal Sains dan Teknologi Mitigasi Bencana*, 15(1), 63–73. <https://doi.org/10.29122/jstmb.v15i1.4114>
- Vieira, L.V., Rodrigues, F.H., & Abel, M. (2020). Ontological Analysis of Weathering. *Proceedings of the XIII Seminar on Ontology Research in Brazil and IV Doctoral and Masters Consortium on Ontologies (ONTOBRAS 2020) Vitória, Brazil, November 23-26, 2020*, pp.134–147. <https://ceur-ws.org/Vol-2728/paper10.pdf>